In silico muscle volume conduction study validates in vivo measurement of tongue volume conduction properties using the UTA depressor

Xuesong Luo[1] **and Benjamin Sanchez**[1]‡

[1]Sanchez Research Lab, Department of Electrical and Computer Engineering, University of Utah, Salt Lake City, UT 84112-9206, USA.

E-mail: benjamin.sanchez@utah.edu

Abstract. *Objective*: Electrophysiological assessment of the tongue volume conduction properties (VCPs) using our novel multi-electrode *user tongue array* (UTA) depressor has the promise to serve as a biomarker in patients with bulbar dysfunction. However, whether in vivo data collected using the UTA depressor accurately reflect the tongue VCPs remains unknown. *Methods*: To address this question, we performed in silico simulations of the depressor with an accurate anatomical tongue finite element model (FEM) using healthy human tongue VCP values –namely the conductivity and the relative permittivity– in the sagittal plane (i.e., longitudinal direction) and axial and coronal planes (i.e., transverse directions). We then established the relationship between tongue VCP values simulated from our model to measured human data. *Results*: Experimental versus simulated tongue VCP values including their spatial variation were in good agreement with differences well within the variability of the experimental results. *Conclusions*: Tongue FEM simulations corroborate the feasibility of our UTA depressor in assessing tongue VCPs. *Significance*: The UTA depressor is a new non-invasive and safe tool to measure tongue VCPs. These electrical properties reflect tongue's ionic composition and cellular membrane integrity and could serve as a novel electrophysiological biomarker in neurological disorders affecting the tongue.

Keywords: tongue, muscle volume conduction study, volume conduction properties, finite element model.

Introduction

Oral muscles related to eating, swallowing and communicating are progressively affected in a host of neurological conditions. For example, approximately 25% of patients with amyotrophic lateral sclerosis (ALS) have speech and swallowing symptoms at the time

‡ Corresponding author: Dr. Benjamin Sanchez, Sorenson Molecular Biotechnology Building, Office 3721, 36 South Wasatch Drive, University of Utah, Salt Lake City, UT 84112-9206, USA, phone: (801) 585-9535, email: benjamin.sanchez@utah.edu.

of disease onset (Yunusova et al. 2019). In addition, bulbar dysfunction is a common manifestation of many other neuromuscular disorders including myasthenia gravis and oculopharyngeal, facioscapulohumeral (Yamanaka et al. 2001), and Duchenne muscular dystrophies affecting both children and adults.

Despite the importance of tongue function to overall quality of life and life expectancy, commonly employed tools for tongue assessment have limitations. The ALS functional rate scale-revised test includes only 3 out of 12 questions to rate the patients level of bulbar impairment in performing speech, salivation, and swallowing tasks. While clinically valuable, the test is based on patient feedback, with limited assessment of bulbar dysfunction which may lead to delayed bulbar impairment assessment and underestimation of disease severity (Smith et al. 2017). Other physiological monitoring tools of bulbar function include maximum tongue pressure testing via pressure transducing tongue depressors; however, values are dependent on the subject' motivation, number of trials, feedback, and tongue and jaw position (Solomon 2004, Hayashi et al. 2002). Craniobulbar muscle health can be assessed using standard needle electromyography (EMG) but, as commonly practiced, data interpretation is subjective (Kendall & Werner 2006, Narayanaswami et al. 2016). Furthermore, tongue EMG has limited sensitivity in detection of pathology in ALS and associated discomfort does not allow EMG to follow disease progression and response to therapy (Gans & Kraft 1977, Jan et al. 1999).

Video fluoroscopic swallowing exam visualizes in real time the patient's ability to swallow safely and effectively various types of barium-containing foods (Briani et al. 1998, Wright & Jordan 1997); however, the test does not provide quantifiable metrics, it requires a specialized facility with expensive instrumentation and highly trained personnel, and there is an associated risk of radiation exposure. State-of-art voice smartphone apps can help detect slowness of the speech mechanism (Stegmann et al. 2020); however, it is a non-tongue specific functional outcome that can be associated to damage to the central or peripheral nervous system or both.

Here, we perform an in silico muscle volume conduction study of the human tongue to evaluate the ability of electrical volume conduction of the bulk of the tongue. Tongue volume conduction properties (VCPs) measured during a tongue volume conduction study are the conductivity –which quantifies the ease with which electric charge is transported through the bulk of the tongue muscle– and the relative permittivity – which quantifies the ability of tongue muscle to store and release electromagnetic energy– (Sanchez et al. 2021). These physical material properties are objective and quantitative on an standardized scale and they are determined by the ionic concentration and membrane integrity, both physiological features of muscle altered in a wide variety of neuromuscular disorders (Nagy et al. 2019). For example, an increase of the ionic concentration of the extracellular medium would expect to increase the conductivity of the bulk of the muscle. The gold standard method for measuring the muscle VCPs requires a biopsy procedure (Sanchez et al. 2014); however, due to the invasiveness, the technique has limited clinical use. Another important limitation of biopsy is the

inability to follow the natural progression of muscle VCPs with disease because of inherent sampling limitations.

We have created a novel non-invasive tongue depressor technology, called user tongue array (UTA) depressor, that allowed us to measure for the first time in vivo tongue VCPs in healthy volunteers (Luo et al. 2020). Despite our preliminary success in obtaining human data, a question that remains unanswered is whether in vivo data collected using our novel UTA depressor accurately reflect human VCPs due to unexpected experimental artifacts. Thus, here, we performed an in silico study based on a human tongue finite element model (FEM) using our depressor to evaluate the accuracy of our reconstruction algorithm at calculating in vivo the conductivity and relative permittivity of the tongue. We then compared experimental and modeled tongue VCPs values to validate our new technology.

Methods

Tongue finite element model simulations

We simulated a healthy human tongue anatomical FEM based on the VIP-Duke v.3.0 model (DOI: 10.13099/VIP11001-03-0) and spatial resolution of $0.5\times0.5\times0.5$ mm^3 with the depressor positioned on the top surface of the anterior tongue (see Figure 1 A and B). Meshing and electrostatic simulations under quasi-static approximation were performed in Comsol software using the AC/DC Module (Comsol Multiphysics, Burlington, MA) and conjugate gradient iterative solver. Adaptive meshing was used to discretize the tongue conductor volume into small regions or elements based on the electric potential gradient. The mesh included coarse tetrahedral in regions with no electric potential change and fine triangular elements near the electrodes were used. In our simulations, we considered point-like electrodes and did not include electrode impedance contact artifacts since this experimental error source affecting all electrodes would not influence the simulation results (Schwan 1968). For each measuring direction in the depressor 0°, 45°, 90° and 150° (Figure 1 C), we simulated the tongue FEM model applying 100 μA_{rms} across source and sink outer electrodes and then measured the resulting voltage using the second pair of inner sense electrodes. Current and voltage electrodes were arranged in concentric circles with radii 4 and 7 mm, respectively. The current applied conforms to the current limits specified by the IEC-60601 standard for medical devices This measurement procedure was then repeated in all four directions sequentially.

Simulated tongue volume conduction properties

We used averaged healthy in vivo tongue conductivity and relative permittivity values along with their spatial variation –a concept also known as electrical anisotropy (Kwon et al. 2019)– publicly available in our recently completed study (Luo et al. 2020). In that study, we were able to calculate in vivo human anisotropic tongue VCPs from multi-directional surface tongue impedance measurements using a reconstruction algorithm

Figure 1. (A) Three-dimensional view of the tongue finite element model (FEM) with the user tongue depressor. (B) Top view. (C) Top view detail of the FEM dimensions length and width, angular arrangement of the surface electrodes and model mesh.

(see additional details in Data analysis Section). Here, longitudinal conduction values were assigned in the sagittal plane whereas transverse conduction values were assigned in both the axial and coronal planes.

Impedance sensitivity analysis

We performed a sensitivity analysis to determine the tongue depth measured by the depressor from FEM simulations as described in (Rutkove et al. 2017). The sensitivity distribution in the tongue was calculated as $S = J_1 \cdot J_2$ (m^{-4}), where $J_{1,2}$ are the local current density in m^{-2} vectors resulting from the application of an electric current between the two electrodes in the outer circumference and the other two electrodes in the inner circumference.

Data analysis

The electrodes' spacing and direction along with simulated apparent surface tongue impedance values (resistance and reactance) obtained in each direction were used by the reconstruction algorithm described in (Kwon et al. 2017) to calculate two-dimensional anisotropic in vivo conductivity and relative permittivity values of the tongue. The underlying assumption of the algorithm is the tongue volume can be considered as semi-infinite (i.e., half-space) volume where the electrical current can flow without boundary interference. To assess the impact of this assumption when simulating a realistic human tongue FEM model, original (i.e., obtained from human experiments used in our simulations) and reconstructed (i.e., obtained from inverting tongue FEM simulations) tongue conductivity and relative permittivity results were then compared at the measurement frequencies using MATLAB (The MathWorks, Natick, MA).

Results

FEM current density and electric potential distribution within the tongue

Adaptive mesh resulted into 464,269 model elements, which allowed us to have an accurate and realistic spatial current and electric potential distribution simulation while

keeping the simulation time reasonably low (∼15 s using 2.2 GHz 6-core i7-8750H processor and 24 GB of DDR4 RAM memory at 2666 MHz). Figure 2 shows a model simulation at 8 kHz with the current flowing from the source and sink electrodes located in the depressor at 0° direction. Figure 2 provides a qualitative representation of the current flow through the tongue. As expected, the current generates greater isopotential surfaces underneath the electrodes and less at a greater depth where the current density is less. Note this qualitative current simulation does not allow determination of the measurement depth. For this, a quantitative study based on a sensitivity analysis is performed next.

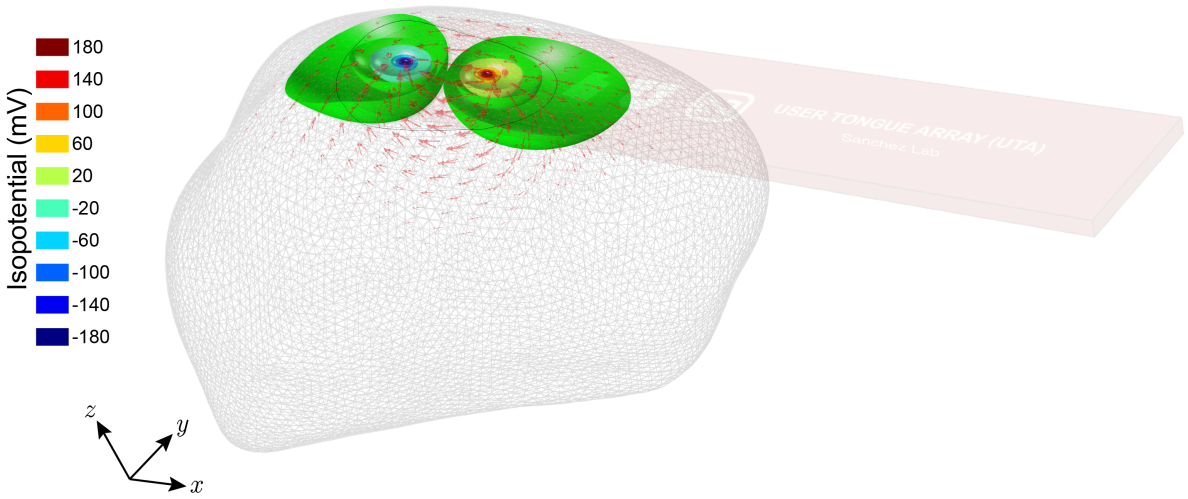

Figure 2. Representative electrostatic simulation for measuring the volume conduction properties of the tongue at 8 kHz and 0°. For each measurement direction 0°, 45°, 90° and 150° and frequency 8, 16, 32, 64, 128 and 256 kHz measured, electric current is applied through the corresponding outer sink and source electrodes (the current distribution within the tongue is shown in red arrows), whereas the inner electrodes record the voltage resulting from the isopotential surfaces generated within the tongue. The length of the current arrows indicates the amplitude of current at each point within the tongue.

Tongue measurement depth

Figure 3 A shows the tongue region measured with our depressor. This colored sensitivity region corresponds to an arbitrary defined 99.9% of the measured sensitivity contributing to the measured VCP data. In other words, the expected contribution of anatomical features including tissues and fluids outside this region is less than 0.1%. As illustrated in more detail in Figure 3 B and C, the measurement region is underneath the depressor and the maximum depth is 13.3 mm.

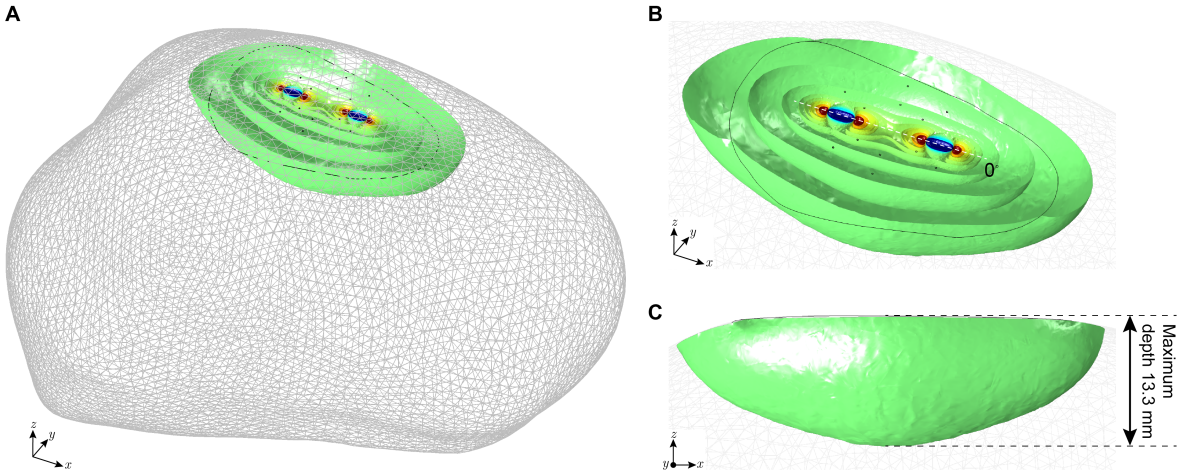

Figure 3. (A) Three-dimensional sensitivity simulation shows the volume measured of the tongue using our depressor. Regions on the tongue outside the simulated sensitivity volume are not measured. (B) Detail. (C) Side view to determine the maximum depth of measurement. Simulation details: 8 kHz frequency and 0°.

Experimental and simulated tongue volume conduction properties values

Figure 4 plots experimental versus simulated conductivity and relative permittivity tongue VCP values in longitudinal and transverse directions at all frequencies. Simulated tongue VCP values are within the variability of real human tongue VCPs data. For example, experimental (mean±standard error of the mean) longitudinal and transverse conductivity values at 8 kHz are 0.37±0.1 (N=4) and 0.17±0.02 (N=4) versus FEM simulated 0.34 and 0.17 S m^{-1}, respectively. Similarly, longitudinal and transverse relative permittivity values at 8 kHz are $(10.5\pm6.5)\cdot10^5$ (N=6) and $(4.6\pm3.0)\cdot10^5$ (N=6) versus FEM simulated $9.5\cdot10^5$ and $4.6\cdot10^5$, respectively.

Discussion

As part of our ongoing research, we have recently tested our UTA depressor and reported for the first time in vivo values measuring tongue VCPs including their directional dependence in a small group of healthy volunteers performing measurements on themselves (Luo et al. 2020). These VCPs of the tongue provide quantitative, objective and standardized data reflecting anomalous electrical and physical behavior of molecules in diseased tongue (Duck 1990), for example, due to replacement of healthy muscle tissue with connective and interstitial fat tissues. However, due to the novelty, we still did not know how feasible was actually to measure accurately tongue VCP values in vivo using our UTA depressor. Thus, here we perform a formal verification based on a FEM simulation process. This well-controlled and accurate FEM simulation environment allowed us to discard technical errors that could have affected our experimental measurements.

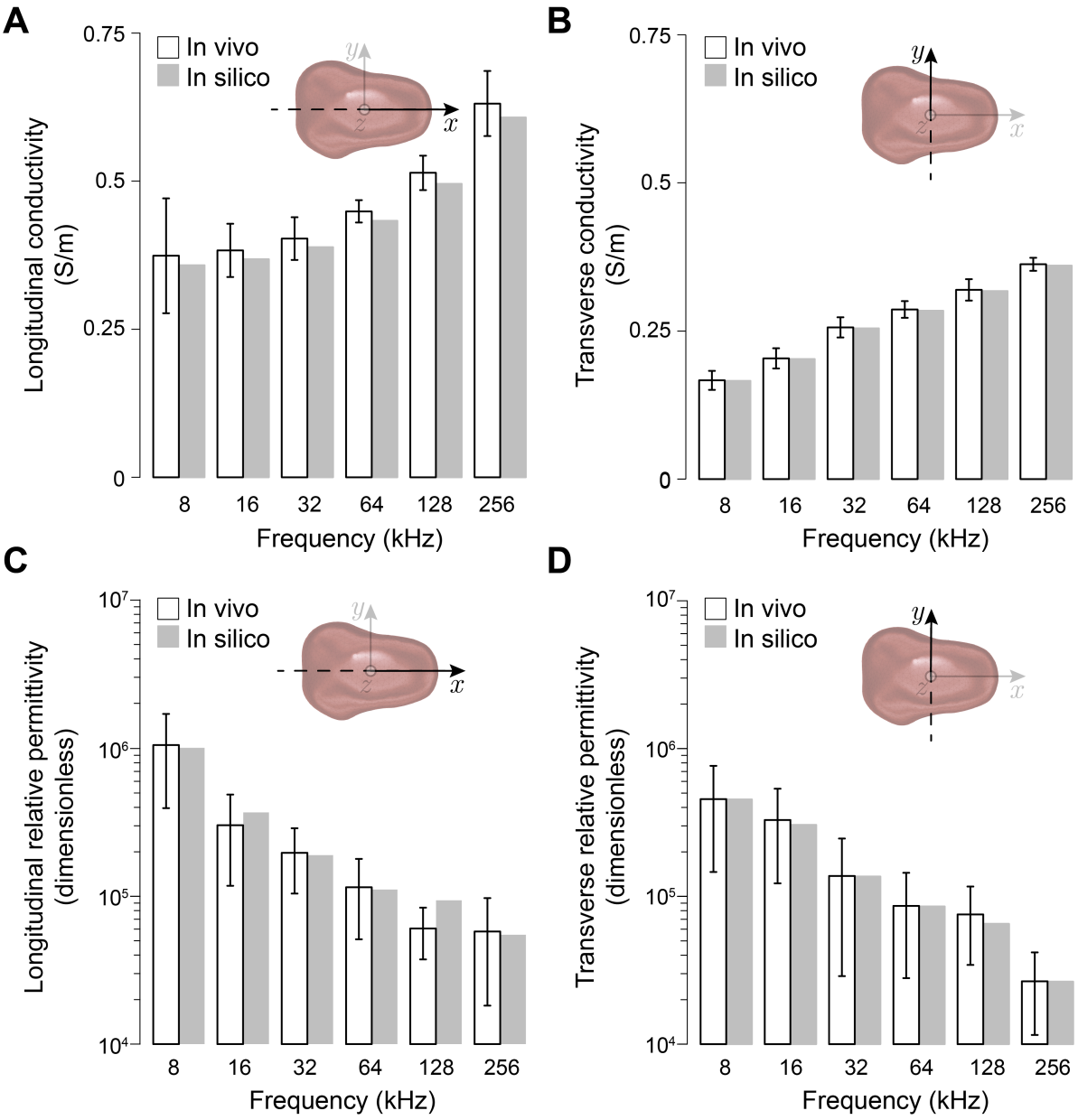

Figure 4. Comparison of in vivo measured human (mean±standard error of the mean) and simulated healthy tongue volume conduction properties. As expected, the trend of conductivity and relative permittivity is increasing and decreasing with frequency, respectively.

These technical errors specifically include assumptions made in the reconstruction algorithm for calculating the conductivity and relative permittivity values from multi-directional apparent tongue impedance values. The reconstruction algorithm was developed on the strict assumption that the conductor volume is *semi-infinite*, in practice, not influenced by the irregular finite-shape of the human tongue. Here, we use FEM simulations to validate or discard this assumption. If the original and the reconstructed conductivity and relative permittivity values were not in good

agreement when simulating an accurate and realistic human tongue FEM model, then our UTA technology most likely would not produce accurate in vivo conductivity and relative permittivity human tongue values. Contrary, the original and reconstructed conductivity and relative permittivity values are in good agreement which indicates our approach is minimally influenced by artifacts introduced by the finite-shape of the tongue. Indeed, assuming a 99.9% volume contributing to the measured sensitivity, the expected the tongue measurement depth is 13.3 mm, which confirms that the technique is robust to substantial tongue atrophy, for example, occurring in patients with bulbar impairment in advanced stages of ALS or fascioscapulohumeral dystrophy (Yamanaka et al. 2001). The overall agreement between experimental and simulated results at the frequencies measured corroborate the validity of our technology for in vivo measurement of human tongue VCPs.

Related to this work, previous studies used the technique of electrical impedance myography (EIM) to evaluate tongue health using a basic 4-electrode handmade popsicle (Sanchez & Rutkove 2017, Rutkove & Sanchez 2018). The authors detected significant differences in EIM phase and resistance values between healthy and ALS patients (Shellikeri et al. 2015, Mcilduff et al. 2017), with the advantage of phase over resistance values of not depending on the spacing between electrodes (Sanchez et al. 2016). However, the underlying mechanism producing such observed EIM effects was not clear due to an overlap of physiological factors including merely simple tongue atrophy and changes in the underlying VCPs of the tongue. A subsequent FEM study attempted to disentangle these two but the interpretation made of the results is questionable due the lack of agreement between experimental and simulated EIM results with differences of about 50% (Pacheck et al. 2016). There are two plausible reasons for such discrepancy. First, the use of an overly simplistic FEM of the human tongue of which the measurement depth was not determined. Second, the use of tongue VCPs values from ex vivo gastrocnemius muscle in a murine model of ALS. A large body of work has shown tissues' VCPs change, among others, within animal species (Schwan & Kay 1956, Geddes & Baker 1967, Pethig 1987) and measured ex vivo versus in vivo (Surowiec et al. 1986, Schaefer et al. 2002). More recently, researchers from the University of Sheffield have measured patients with ALS using a tweezer-like EIM tongue probe with four electrodes both at the upper and lower plates (Alix et al. 2020). A recent FEM study from the same group aimed at evaluating the feasibility to detect lateral asymmetry in affecting the tip of the tongue in ALS (Schooling et al. 2020). Unlike (Pacheck et al. 2016), the authors modeled human tongue impedance values in their simulations.

As reviewed in (Sanchez et al. 2021), the hypothesis supporting the application EIM for neuromuscular evaluation is that alterations affecting the VCPs of diseased muscle can be interrogated indirectly by measuring muscle electrical impedance data (i.e., resistance and reactance). Unlike other probe designs, the UTA depressor and associated algorithm provides the underlying VCPs of the tongue and these are true electrical properties that provide quantifiable, objective, standardized data on a universal scale

and thus are not impacted by electrode distances.

Here, we performed a head-to-head comparison of in vivo experimental and FEM simulated healthy human tongue VCP values including their spatial variation. Despite the good agreement between results which indicates no interference from the finite-shape of the tongue, there are associated inherent limitations to our simulation study. First, the tongue model does not include other muscles beyond the genioglossus muscle or include sublingual arteries and veins. Our simulations indicate, however, that these structures are deeper than depressor' measurement depth and thus their expected is minimal. Second, we simplified the geometric dependency of the genioglossuss myofibers in our model longitudinally and transversely only, whereas the complete three-dimensional myoarchitecture of the human tongue also includes vertically-aligned fibers (Gaige et al. 2007). However, to the best of the authors' knowledge, we are not aware of these anisotropic data being available in the literature. Third, we intentionally omitted the simulation of diseased tongue conditions because currently there is no in vivo human tongue VCP data available including their directional dependence that could be used to perform a realistic and accurate study.

Conclusions

In summary, this simulation study supports our novel non-invasive UTA depressor technology for measuring in vivo tongue VCPs. The results presented support further application of our technology to determine the performance as a diagnostic and longitudinal electrophysiological biomarker for evaluating neurological disorders affecting the tongue. We are currently using our depressor to broader the application to tongue assessment.

Conflict of interest statement

Dr. Sanchez has equity and serves a consultant and scientific advisor to, Haystack Dx, Inc. and Ioniq Sciences, Inc., he is also a member of the companies Board of Directors. Haystack Dx has an option to license patented impedance technology of which Dr. Sanchez is named as an inventor. He also serves as a consultant to Myolex, Inc., Impedimed, Inc., Texas Instruments, Inc., and Happy Health, Inc., companies that develop impedance related technology for consumer, research and clinical use.

Acknowledgments

This work was funded by the China Scholarship Council grant 201906020024 (XL) and National Institutes of Health grant R41 NS112029-01A1 (BS).

1. References

Alix J J, McDonough H E, Sonbas B, French S J, Rao D G, Kadirkamanathan V, McDermott C J, Healey T J & Shaw P J 2020 *Clin. Neurophysiol.* **131**(4), 799–808.

Briani C, Marcon M, Ermani M, Costantini M, Bottin R, Iurilli V, Zaninotto G, Primon D, Feltrin G & Angelini C 1998 *J. Neurol.* **245**(4), 211–216.

Duck F A 1990 *in* 'Phys. Prop. Tissues' Elsevier pp. 167–223.

Gaige T A, Benner T, Wang R, Wedeen V J & Gilbert R J 2007 *J. Magn. Reson. Imaging* **26**(3), 654–661.

Gans B M & Kraft G H 1977 *Arch. Phys. Med. Rehabil.* **58**(1), 13–6.

Geddes L A & Baker L E 1967 *Med. Biol. Eng.* **5**(3), 271–293.

Hayashi R, Tsuga K, Hosokawa R, Yoshida M, Sato Y & Akagawa Y 2002 *Int. J. Prosthodont.* **15**(4), 385–8.

Jan M M, Schwartz M & Benstead T J 1999 *Can. J. Neurol. Sci.* **26**(4), 294–297.

Kendall R & Werner R A 2006 *Muscle Nerve* **34**(2), 238–41.

Kwon H, de Morentin M M, Nagy J A, Rutkove S B & Sanchez B 2019 *Physiol. Meas.* **40**(8), 085008.

Kwon H, Nagy J A, Taylor R, Rutkove S B & Sanchez B 2017 *Phys. Med. Biol.* **62**(22), 8616–8633.

Luo X, Gutierrez Pulido H V, Rutkove S B & Sanchez B 2020 *Clin. Neurophysiol.* **20**(30555-1), S1388–2457.

Mcilduff C E, Yim S J, Pacheck A K & Rutkove S B 2017 *Muscle Nerve* **55**(4), 539–543.

Nagy J A, DiDonato C J, Rutkove S B & Sanchez B 2019 *Sci. Data* **6**(1), 37.

Narayanaswami P, Geisbush T, Jones L, Weiss M, Mozaffar T, Gronseth G & Rutkove S B 2016 *Neurology* **86**(3), 218–223.

Pacheck A, Mijailovic A, Yim S, Li J, Green J R, McIlduff C E & Rutkove S B 2016 *Clin. Neurophysiol.* **127**(3), 1886–1890.

Pethig R 1987 *Clin. Phys. Physiol. Meas.* **8 Suppl A**, 5–12.

Rutkove S B, Pacheck A & Sanchez B 2017 *Muscle Nerve* **56**(5), 887–895.

Rutkove S B & Sanchez B 2018 *Cold Spring Harb. Perspect. Med.* p. a034405.

Sanchez B, Li J, Bragos R & Rutkove S B 2014 *Phys. Med. Biol.* **59**(10), 1–12.

Sanchez B, Martinsen O G, Freeborn T J & Furse C M 2021 *Clin. Neurophysiol.* **132**(2), 338–344.

Sanchez B, Pacheck A & Rutkove S B 2016 *Sci. Rep.* **6**(1), 32615.

Sanchez B & Rutkove S B 2017 *Curr. Neurol. Neurosci. Rep.* **17**(11), 86.

Schaefer M, Gross W, Ackemann J & Gebhard M M 2002 *Bioelectrochemistry* **58**(2), 171–80.

Schooling C N, Jamie Healey T, McDonough H E, French S J, McDermott C J, Shaw P J, Kadirkamanathan V & Alix J J 2020 *Physiol. Meas.* .

Schwan H & Kay C 1956 *Circ. Res.* **4**(6), 664–670.

Schwan H P 1968 *Rev. Sci. Instrum.* **39**(4), 481.

Shellikeri S, Yunusova Y, Green J R, Pattee G L, Berry J D, Rutkove S B & Zinman L 2015 *Muscle Nerve* **52**(4), 584–91.

Smith R, Pioro E, Myers K, Sirdofsky M, Goslin K, Meekins G, Yu H, Wymer J, Cudkowicz M, Macklin E A, Schoenfeld D & Pattee G 2017 *Neurotherapeutics* **14**(3), 762–772.

Solomon N P 2004 *Int. J. Orofac. Myol.* **30**, 8–19.

Stegmann G M, Hahn S, Liss J, Shefner J, Rutkove S, Shelton K, Duncan C J & Berisha V 2020 *npj Digit. Med.* **3**(1), 132.

Surowiec A, Stuchly S S & Swarup A 1986 *Bioelectromagnetics* **7**(1), 31–43.

Wright R & Jordan C 1997 *Palliat. Med.* **11**(1), 44–48.

Yamanaka G, Goto K, Matsumura T, Funakoshi M, Komori T, Hayashi Y K & Arahata K 2001 *Neurology* **57**(4), 733–735.

Yunusova Y, Plowman E K, Green J R, Barnett C & Bede P 2019 *Front. Neurol.* **10**, 106.